ORIGINAL PAPER

Identification of material parameters of a shear modified GTN damage model by small punch test

Quan Sun · **Yebo Lu** · **Jianjun Chen**

Abstract A new approach was put forward to identify the damage parameters of the shear modified GTN damage model proposed by Nahshon and Hutchinson (Eur J Mech Solid 27:10–17, 2008) by combining the artificial neural networks algorithm and small punch test. The factorial design method was used to analyze the influence of the parameters on the shape of load-displacement curve of small punch test. The less important parameters were set as empirical value and the significant factors were determined by an artificial neural networks model which was build up based on large amount of simulations of small punch tests with different levels of damage parameters values. The identified parameters were validated by small punch test simulations with different specimen thickness. The results show that the identified parameters of the shear modified GTN damage model are effective to characterize the mechanical behavior as well as the damage evolution and ductile failure of material during the process of small punch test. In addition, the applicability of the identified parameters in the tests with different stress condition were verified.

Q. Sun (✉) · Y. Lu
School of Mechanical and Electrical Engineering, Jiaxing University, Jiaxing 314001, China
e-mail: sunquan0501@163.com

J. Chen
School of Mechanical and Power Engineering, East China University of Science and Technology, Shanghai 200237, China

1 Introduction

It is well known that the process of ductile failure of materials involves three stages: (1) nucleation of micro-voids by either fracture or decohesion of the second-phase particles and inclusions, (2) volume growth of micro-voids induced by plastic straining, (3) coalescence of enlarged voids due to plastic flow localization and final tearing of the ligaments between enlarged voids when the voids volume fraction reaches a critical value. The constitutive model proposed by Gurson (1977) is the most well-established damage theory that describes the ductile failure of metal materials caused by the growth of micro-voids. Afterwards, Gurson's model has been improved by several researchers. The extension proposed by Tvergaard and Needleman (1984), commonly referred to as GTN damage model, has achieved widespread acceptance within the scientific community.

However, there are two main shortcomings that prevent the GTN damage model from being widely used in the simulation of engineering problems. Firstly, the good performance of the GTN damage model in the predicting of material fracture depends on precise knowledge of its nine constitutive parameters (q_1, q_2, q_3, f_0, f_N, ε_N, S_N, f_c, f_F) associated with the material. The experimental determination of

the material parameters is very complex. One principal approach to identify these parameters is using the inverse method coupled with non-linear optimization procedure. The principle of inverse method is to quantitatively describe the complicated stress–strain responses and minimize the difference between the test results and the corresponding numerical simulation results by using an advanced optimization technique. Corigliano et al. (2000) solved the inverse problem of parameters identification via the extended Kalman filter for nonlinear systems coupled with a numerical methodology for the sensitivity analysis. Springmann and Kuna (2005, 2006) identified the parameters by using a gradient-based optimization procedure to fit the experimental and numerical calculated forces at given displacements based on the quadratic approximation. Muñoz-Rojas et al. (2010) determined the parameters by inverse analysis using genetic algorithms. Since the inverse method is based on large amounts of finite element computation to adjust the parameters step by step via non-linear optimization procedure, it usually requires prohibitive computing time and cost to get the proper parameters.

Another important approach to calibrate the GTN parameters is using the artificial neural networks (ANN) which builds the relationships between the stress–strain response or load-displacement curve of a certain material mechanical test and the GTN model parameters. First, the simulation results of the material mechanical test with different damage parameters values were used to train the ANN, and then the parameters can be identified via the well trained ANN based on the experimental results of the material mechanical test. The small punch test (SPT) Abendroth and Kuna (2003), Abendroth and Kuna (2006), sheet metal blanking Aguir and Marouani (2010), Marouani and Aguir (2012) and notched tensile Abbassi et al. (2013) were used by many researchers to calibrate the damage parameters of GTN model. Although the training of ANN relies on a number of numerical results with varying GTN model parameters, the ANN approach requires much less computing time compared with the classical inverse method Abbassi et al. (2013).

Secondly, many recent studies have shown that the GTN damage model is inapplicable to predict localization and fracture for some ranges of stress triaxiality Nahshon and Hutchinson (2008). Under tensile loading condition, which corresponds to high values of stress triaxiality, the material damage behavior is dom-

inated by voids nucleation, growth and coalescence which can be characterized by GTN damage model. However, under shear loading condition, the governing failure mechanism is characterized by the shear localization of plastic strain of the inter-voids ligaments caused by voids rotation and distortion Barsoum and Faleskog (2007). Since the GTN damage model does not include those important phenomena, it is unable to capture the real damage behavior of materials under those conditions. Some significant improvements in the damage evolution mechanism have been made based on phenomenological or geometrical considerations to overcome this limitation. The most popular one is the shear modified GTN model coupled with shear damage mechanism proposed by Nahshon and Hutchinson (2008), which has been widely used to characterize the ductile damage and assess the formability of metals Achouri et al. (2013).

In the shear modified GTN damage model coupled with the Nahshon and Hutchinson shear damage mechanism, a new constitutive parameter, which defines the magnitude of the damage growth rate in shear stress state, is introduced, which makes the identification of GTN model parameters more complex. In the present paper, a set of methods is established to identify the shear modified GTN parameters by small punch test. Firstly, the fractional factorial design was used to minimize the number of the damage parameters of the shear modified GTN model which need to be calibrated while some of them have little effect on the stress–strain response of material. Then, the parameters are identified by means of ANN method based on experiments and simulations of small punch test. At last, the reliability of the determined parameters based on the current method were verified by SPTs with different specimen thickness.

2 Experimental method

The small punch test (SPT) is a mechanical testing method that has been widely used in recent decades. In the SPT, a disk like specimen of $\varnothing 10 \times 0.5$ mm size is deformed in a miniaturized deep drawing experiment. Fig. 1 shows the principle sketch of the SPT with the essential geometric measures. The specimen is clamped between the lower and upper dies and deforms until fracture driven by the punch via a rigid ball with a diameter of $D = 2.4$ mm. While the hole in the lower
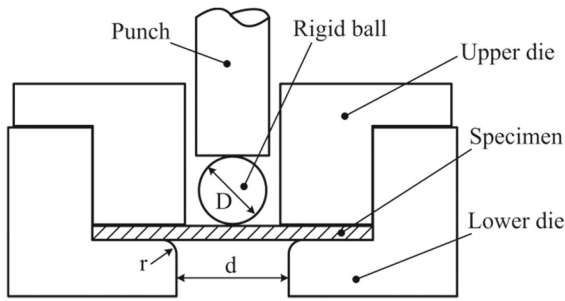
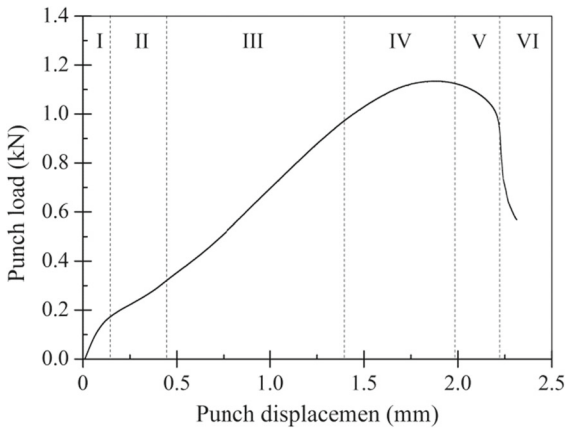**Fig. 1** Principle sketch of the small punch test

Fig. 2 Stages in load-displacement curve of SPT

die has a diameter of $d = 4$ mm and a fillet radius of $r = 0.5$ mm.

The measurable output of the SPT is the load-displacement curve of the punch which contains information about the elastic-plastic deformation behavior and strength and fracture properties of the material. The typical load-displacement curve for a ductile metallic material is shown in Fig. 2. In general, the curve can be divided into several parts. Part I is mainly the elastic response of the material. Part II reflects the transition from elastic to plastic behavior. Part III shows the hardening properties during large plastic deformation. In part IV, the damage begins to make a difference and softening occurs. Part V describes the rapid decrease of material load carrying capacity as damage reaches a critical value and final fracture happens in Part VI.

Figure 3 presents the result of the small punch specimen after fracture. The SEM observation on the fracture surface indicates that the failure of the specimen is the result of ductile damage which is characterized by voids nucleation and volume growth. In addition, the voids

shape in the dimple structure shows that voids shape distortion also plays an important role in the damage and fracture of specimen in SPT.

3 Numerical simulation

3.1 Finite element model

In this work, the SPT was simulated by finite element software ABAQUS. Since the geometrical and the load of SPT are axisymmetric, a two-dimension finite element model was constructed as shown in Fig. 4. The specimen was meshed with axisymmetric reduced integration elements. Different element sizes have applied to check the mesh dependency on the simulation results and finally the mesh size of about 0.1 mm × 0.1 mm was applied and mesh refinement of 0.06 mm × 0.1 mm was performed in the specimen center where the plastic deformation and damage was located. The die, down-holder and punch ball are modeled as rigid bodies. Die and down-holder are fixed in all degrees of freedom, whereas the rigid ball can moved vertically by a displacement boundary condition. The contact between specimen and rigid ball, die and down-holder is modeled including penalty friction with friction coefficient is 0.2.

3.2 Material model

The GTN damage model coupled with shear damage mechanism Nahshon and Hutchinson (2008) was used to simulation the plasticity, damage fracture behavior of the SPT. The yield surface of GTN damage model can be described as following:

$$\phi\left(\sigma_{ij}, \bar{\sigma}, f^*\right) = \left(\frac{\sigma_{eq}}{\bar{\sigma}}\right)^2 + 2f^* q_1 \cosh\left(-\frac{3q_2\sigma_m}{2\bar{\sigma}}\right)$$
$$-1 - q_3\left(f^*\right)^2 = 0 \qquad (1)$$

where $\sigma_{eq} = \sqrt{\frac{3}{2}s_{ij}s_{ij}}$ is the macroscopic von Mises equivalent stress, and $\sigma_m = \frac{1}{3}\sigma_{kk}$ is the macroscopic hydrostatic stress. $s_{ij} = \sigma_{ij} - \frac{1}{3}\sigma_{kk}\delta_{ij}$ denotes the deviatoric components of Cauchy stress σ_{ij}, and δ_{ij} is the Kronecker delta. $\bar{\sigma}$ is the flow stress of undamaged material matrix. f^* is the total effective void volume fraction. q_1, q_2 and q_3 are the fitting parameters proposed by Tvergaard Tvergaard (1981, 1982) to better

Fig. 3 Small punch test specimen after fracture and SEM photo of the fracture surface
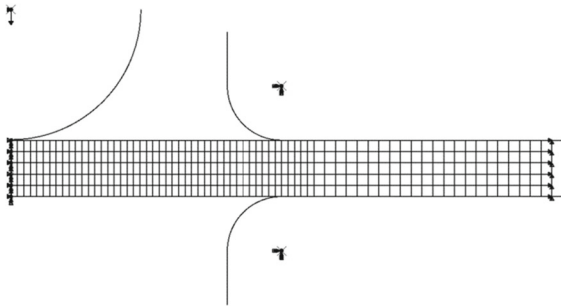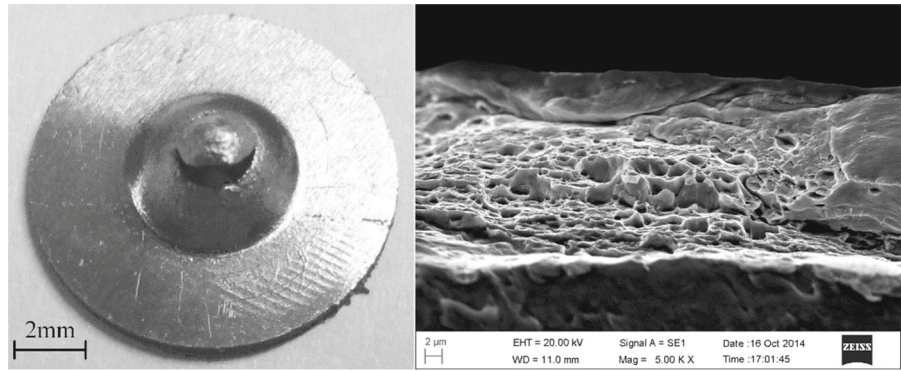

Fig. 4 Finite element model of SPT

represent the void's interaction effects Abendroth and Kuna (2003).

The damage variable f^* is defined as the function of void volume fraction f

$$f^* = \begin{cases} f, & f \leqslant f_c \\ f_c + \kappa(f - f_c), & f > f_c \end{cases} \tag{2}$$

where $\kappa = (f_u - f_c)/(f_F - f)$ is the void growth acceleration factor which represents the rapid drop of material load capacity due to void coalescence. The parameter f_c is the critical void volume characterizing the beginning of coalescence. f_F is the void volume fraction at rupture and $f_u = 1/q_1$ represents the ultimate value of void volume fraction when the material load capacity reduces to zero.

With the shear damage mechanism proposed by Nahshon and Hutchinson (2008), the new expression for the growth rate of void volume fraction is given as:

$$\dot{f} = \dot{f}_g + \dot{f}_n + \dot{f}_s \tag{3}$$

where $\dot{f}_g$, $\dot{f}_n$ and $\dot{f}_s$ represent the growth of pre-existing void, the nucleation of new voids, and the shape change of voids after plastic deformation respectively.

The growth rate of pre-existing voids is controlled by the trace of plastic strain increment tensor.

$$\dot{f}_g = (1 - f)\dot{\varepsilon}_{kk}^p \tag{4}$$

The nucleation of new voids was taken to be governed by normal distribution.

$$\dot{f}_n = \frac{f_N}{S_N\sqrt{2\pi}} \exp\left[-\frac{1}{2}\left(\frac{\bar{\varepsilon}^p - \varepsilon_N}{S_N}\right)^2\right]\dot{\bar{\varepsilon}}^p \tag{5}$$

where f_N is volume fraction of void nucleating particles, ε_N is the mean void nucleation plastic strain and S_N is corresponding deviation of the normal distribution.

The variable f_s is introduced by Nahshon and Hutchinson (2008) consistent with the mechanism of void softening in shear condition and the expression is given as

$$\dot{f}_s = k_s w(\sigma_{ij}) f \frac{s_{ij}\dot{\varepsilon}_{ij}^p}{\sigma_{eq}} \tag{6}$$

where k_s is defined as the magnitude of the damage growth rate in pure shear state. $w(\sigma_{ij})$, the measurement of current stress state, is defined as $w(\sigma_{ij}) = 1 - \left(\frac{27J_3}{2\sigma_{eq}^3}\right)^2$, and $J_3 = \frac{1}{3}s_{ij}s_{jk}s_{ki}$ is a third invariant of stress tensor. The value of $w(\sigma_{ij})$ varies from zero for all axisymmetric stress state ($\sigma_1 = \sigma_2 \geqslant \sigma_3$ or $\sigma_1 \geqslant \sigma_2 = \sigma_3$) to one for a pure shear stress plus a hydrostatic contribution ($\sigma_1 = \sigma_m + \tau$, $\sigma_2 = \sigma_m$ and $\sigma_3 = \sigma_m - \tau$, where $\sigma_1, \sigma_2, \sigma_3$ is the principal stresses with the order $\sigma_1 \geqslant \sigma_2 \geqslant \sigma_3$).

The shear modified GTN damage model was implemented into the commercial finite element code ABAQUS via user-defined material subroutine interface VUMAT. The integration scheme of the constitu-

Table 1 Chemical analysis of the normalizing silicon steel (% in weight)

C	Si	Mn	P	S
0.014	0.367	0.374	0.694	0.040

Table 2 Material elastic-plastic parameters

E (GPa)	v	K	N
201	0.3	690	0.25

tive law of the model is detailed in literature Nahshon and Xue (2009).

3.3 Numerical procedure

To sum up, the shear modified GTN damage model contains ten parameters which can be classified as constitutive parameters (q_1, q_2, q_3) and the material parameters (f_0, f_N, ε_N, S_N, k_s, f_c, f_F). Each of them influences the shape of the load-displacement curve at different stages in the SPT Cuesta et al. (2010): The part I and II of curve are mainly controlled by the elastic-plastic material properties. The influence of initial damage f_0 in this stage is limited and can be ignored. The damage evolution parameters f_N, ε_N, S_N and k_s start their influence in Part III. In this stage, the damage grows with the large plastic deformation, and the curve is controlled by the competition of damage softening and plastic work hardening. The damage softening becomes dominant gradually as the damage grows rapidly in Part IV stage. When the damage reaches a certain high value, the material carrying capacity begins to decrease. Part V is the final failure stage with the macroscopic cracks occurring and extending and the material loses its carrying capacity completely.

4 Parameters identification

4.1 Elastic-plastic behavior

A kind of cold rolled silicon steel, which was widely used in magneto-mechanical engineering, was applied in this study. The chemical compositions are listed in Table 1.

The elastic-plastic material properties were obtained from the true stress–strain curve of uniaxial tensile test. Due to the damage development as strain grows, it is necessary to extrapolate values from undamaged material using the Hollomon law ($\sigma = K\varepsilon^N$) to remove the damage effect on the material elastic-plastic behav-
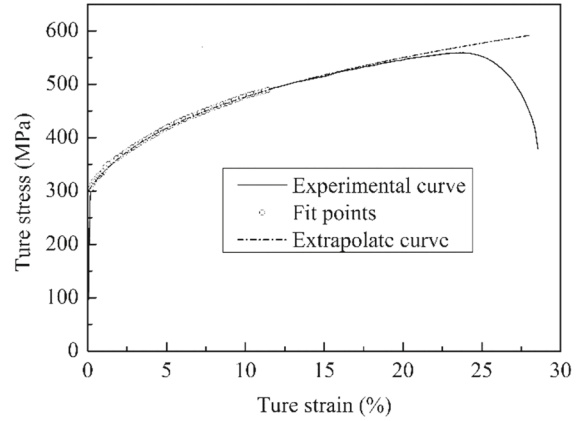

Fig. 5 True stress–strain experimental and extrapolate curve

ior. The true stress–strain experimental and extrapolate curve are shown in Fig. 5 and the elastic and plastic parameters obtained from the stress–strain curve are listed in Table 2

4.2 Fractional factorial design analysis

In most published literatures Benseddiq and Imad (2008), the constitutive parameters q_1, q_2 and q_3 are often fixed as $q_1 = 1.5$, $q_2 = 1.0$ and $q_3 = q_1^2$. There are still seven unknown damage parameters which can be classified as damage evolution parameters: f_0, f_N, ε_N, S_N, k_s and the failure parameters: f_c, f_F. In order to further minimize the number of damage parameters that need to be calibrated, the experimental design methodology was used in this research.

A fractional design with a number of $2^{5-1} = 16$ classes numerical simulations were performed to determine the influencing degree of the damage evolution parameters (f_0, f_N, ε_N, S_N, k_s) on shape of load-displacement curve of SPT. Table 3 shows the levels of the five parameters. The numerical experimental plan is generated using the statistical software Minitab and involves 16 cases as shown in Table 4. Each of the experiments in factorial design was performed by numerical simulation.

Table 3 Factors and levels used in factorial design

Factor	f_0	ε_N	f_N	S_N	k_s
Label	A	B	C	D	E
Low level (−)	0	0.2	0.02	0.01	1
High level (+)	0.002	0.4	0.04	0.1	3

Table 4 The fractional factorial design in coded form with response

Case no.	A	B	C	D	E	Response (variance)
1	−1	−1	−1	−1	1	0.021955
2	1	−1	−1	−1	−1	0.001666
3	−1	1	−1	−1	−1	0.000399
4	1	1	−1	−1	1	0.001892
5	−1	−1	1	−1	−1	0.008287
6	1	−1	1	−1	1	0.077093
7	−1	1	1	−1	1	0.022031
8	1	1	1	−1	−1	0.002152
9	−1	−1	−1	1	−1	0.001160
10	1	−1	−1	1	1	0.040369
11	−1	1	−1	1	1	0.000813
12	1	1	−1	1	−1	0.000684
13	−1	−1	1	1	1	0.073863
14	1	−1	1	1	−1	0.009972
15	−1	1	1	1	−1	0.001784
16	1	1	1	1	1	0.037642

The response of the factorial design is defined as the variance of the load-displacement curve shape. In order to quantify the variance, an additional case of SPT simulation with no damage involved was conducted and the comparison of the load-displacement curve of the no damage case with that of part of the experimental design cases is shown in Fig. 6. Thus, the variance of each experiment can be calculated using the formula as following:

$$S(b_j) = \frac{1}{N} \sum_{i=1}^{N} \left(\frac{F_i(b_j) - F_i^0}{F_i^0} \right)^2 \qquad (7)$$

where the $F_i(b_j)$ and F_i^0 are, respectively, the punch load in experimental case j and in the no damage case at point i, and N is the total number of points. In this work, the point number is selected as 20 with the interval of 0.2 mm at displacement from 0 to 2.0 mm.
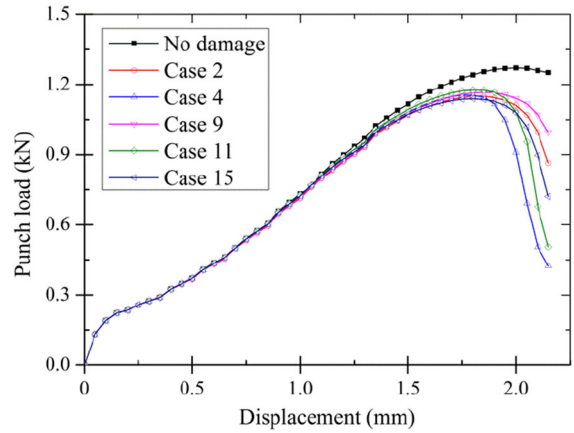
Fig. 6 The comparison of load-displacement curve of SPT simulation between parts of experimental design cases and no damage case
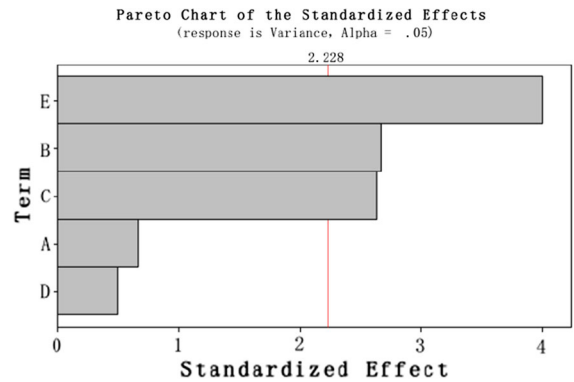

Fig. 7 The Pareto chart of the standardized effects of damage evolution parameters on the shape of load-displacement curve of SPT

The analysis of the factorial design after running the 16 experimental design cases produced the standardized Pareto chart which is presented in Fig. 7. It is a horizontal bar-chart, in which the length of each bar is proportional to the absolute value of its associated estimated standardized effect. The results show that the damage parameters of f_N, ε_N and k_s are important factors that affect the load-displacement curve shape of SPT while the effect of f_0 and S_N is not statistically significant. Thus, the calibration of the five damage evolution parameters can be reduced to three.

The value of S_N is defined as 0.1 which has been used in many studies Benseddiq and Imad (2008), and the initial voids volume fraction f_0 can be estimated according to the material chemical composition using the Franklin formula Ag (1969):

Fig. 8 The identification procedure of material damage parameters using ANN
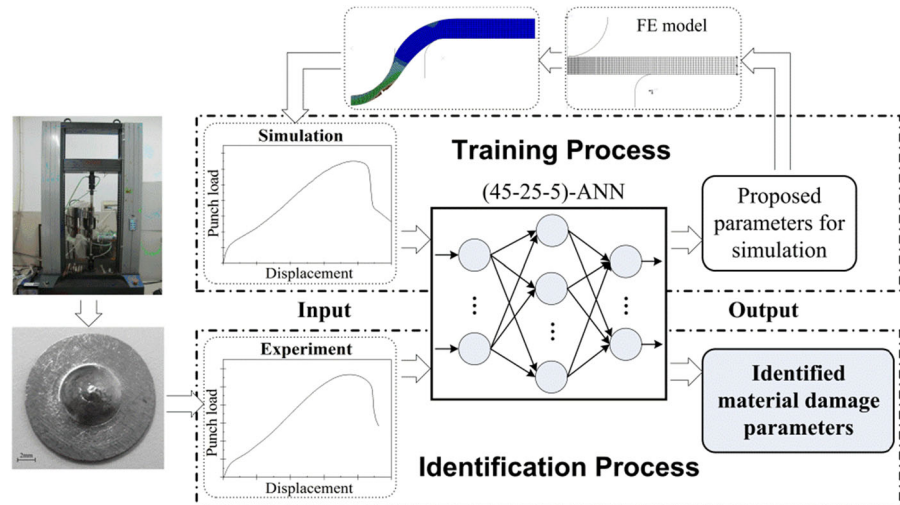
$$f_0 = 0.054 \left(S(\%) - \frac{0.001}{Mn(\%)} \right) = 0.002 \qquad (8)$$

4.3 Artificial neural networks approach

A type of feed forward trained by back-propagation artificial neural networks was used in this work to identify the material damage parameters of the shear modified GTN model. It is able to generate an approximate function for the parameters depending on the shape of the load-displacement curve of SPT. The ANN contains three layers of neurons: the input layers, hidden layer and output layer.

For an ANN including N neurons in the input layer noted as $x_j(j = 1, 2, 3 \ldots N)$, each neuron in the hidden layer receives total outputs from the input layer can be determined as:

$$u_j = \sum_{i=1}^{N} w_{ij} x_i + b_j \qquad (9)$$

where u_j is the potential input to the neuron j in the hidden layer; w_{ij} is the weight from the neuron i in the input layer to neuron j in the hidden layer; b_j is the bias of the neuron j.

The output of a neuron in the hidden layer is computed by applying the potential input to a transfer function. For the feed forward type of ANN, the sigmoid function is usually used as transfer function. So it can be expressed as:

$$y_j = f(u_j) = \frac{1}{1 + \exp(-u_j)} \qquad (10)$$

where y_j is the output from the j neuron in the hidden layer. The computation of the input values and output values of the neurons in the output layer are similar to equation (9) and (10), respectively.

The ANN is trained based on the comparison between the actual and target output, until the actual network output matches the target output. For the back-propagation algorithm, the weights and biases of network were updated in the direction where the performance function (the global error) decreases most rapidly. The error signal $e_i(n)$ at the output of neuron i at iteration n and the sum of squared errors $E(n)$ at iteration n are defined as:

$$E(n) = \frac{1}{2} \sum_{i=C} [t_i - a_i(n)]^2 \qquad (11)$$

where, the set of C includes all the neurons in the output layer of the network, t_i is the target output for the neuron i, and $a_i(n)$ is the actual output of the neuron i at iteration n.

The (45-25-5) ANN model was developed with MATLAB software. In the input layer, there are 45 neurons that represent the 45 values measured for the load evolution versus the displacement of punch in SPT simulation. In the hidden layer, 25 neurons were applied. The 5 damage parameters of f_N, ε_N k_s and f_c f_F were set as 5 neurons in the output layer.

The identification procedure using the ANN model structure is illustrated in Fig. 8. The first step is to train the ANN model. For this purpose, a database of SPT simulation with different values of damage parameters was generated. The variation of the damage parame-

Table 5 Proposed damage evolution parameters for simulation

Parameters	ε_N	f_N	k_s	f_c	f_F
Lower (20%)	0.24	0.2	1.2	0.16	0.24
Normal level	0.3	0.25	1.5	0.20	0.30
Upper (+ 20%)	0.36	0.3	1.8	0.24	0.36

Table 6 Identification results of the damage parameters

Fixed parameters					Identified parameters by ANN				
q_1	q_2	q_3	f	S_N	ε_N	f_N	k_s	f_c	f_F
1.5	1.	2.25	0.002	0.1	0.344	0.217	1.22	0.234	0.351
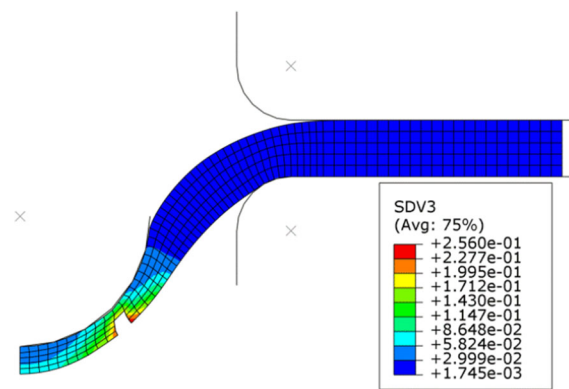
Fig. 9 Simulation results of damage in the specimen of SPT, SDV3 denotes the damage variable f^*

ters is shown in Table 5, and a full factorial design was applied. The total number of finite element simulations is $3^5 = 234$ as 5 parameters and 3 levels for each parameter were considered. The ANN model was trained using 211 (90%) simulations data and the left 10% was applied as validation set to check the accuracy of the ANN model.

Then, in the identification step, the 45 values in load-displacement curve obtained from SPT experiment were applied as 45 input neurons to identify the damage parameters using the trained ANN model.

5 Results and discussion

Table 6 presents the identification results of the damage parameters of the experimental material. In order to verify the identification results, those parameters are used to simulate the SPT. Figure 9 shows the simulation
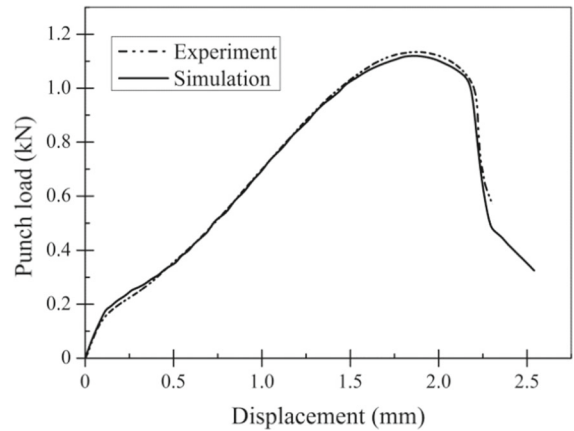

Fig. 10 Comparison between simulation result using identified damage parameters and experiment
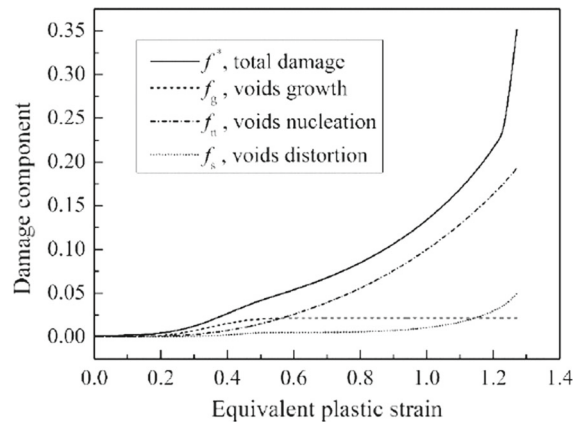

Fig. 11 Evolution of damage component versus the equivalent plastic strain of fracture area in specimen during the process of SPT

results of damage distribution in the specimen. Crack initiates on the button side of specimen about 1 mm out of the center and grows across the specimen until complete fracture. The same position of fracture can be seen in the experiment as shown in Fig. 3. The comparison of load-displacement curve with the simulation and experiment is presented in Fig. 10. The agreement of the two curves indicates that the identified damage parameters of the shear modified GTN damage model are effective to characterize the damage evolution and ductile failure in the SPT. Fig. 11 is the damage evolution versus the equivalent plastic strain of fracture area of specimen during the process of SPT. It can be seen that the voids volume growth is the main factor that contributes to total damage development; however, the
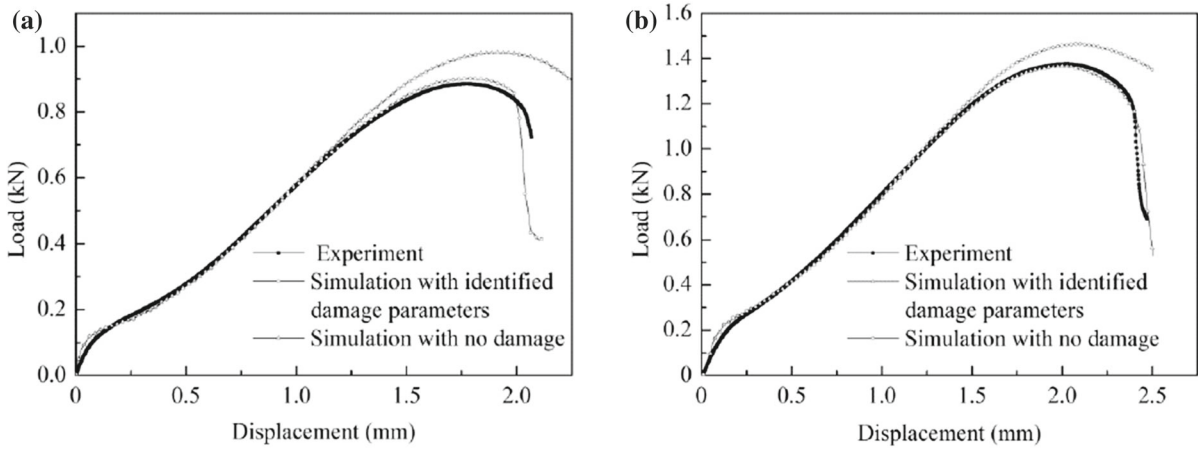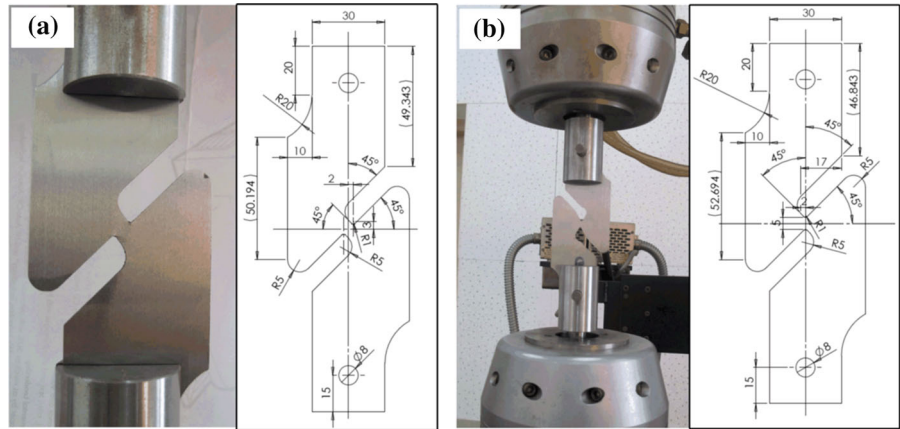
Fig. 12 Experimental and simulation results of SPT curve with specimen thickness of **a** 0.45 mm and **b** 0.55 mm

Fig. 13 Two types of tests: **a** tensile-shear combine testing and **b** pure shear testing

shear damage mechanism caused by the voids shape distortion also plays an important role especially in the final stage where the total damage is relatively high.

In order to further verify those parameters, numerical simulations of SPT with different specimen thickness were conducted. Fig. 12 shows the result curves of experiment and simulation with specimen thickness of 0.45 mm and 0.55 mm. Both the results show that the identified damage parameters of the shear modified GTN model can characterize the material mechanical behavior at a relatively high accuracy during the process of SPT.

In addition, two types of tensile-shear tests shown in Fig. 13a, b were carried out on the universal tensile testing machine to verify the effectiveness of the identified parameters in the material test with different stress condition. The load-displacement curves obtained by numerical simulations with the identified damage parameters were compared with the experiments in Fig. 14. The results of the tensile-shear combine testing shows a good agreement between simulation and experiment; however, it does not agree well in the shear testing, which indicates that the material damage parameters obtained by a specific testing may not be applicable to ones with different stress condition. In the tensile-shear combine testing, shear stress exists in the deformation area at the beginning of the test, however, tensile stress begins to dominate with the increase of deformation and rotation of the deformation zone. The stress condition is similar to that of SPT in a certain way, which may be the reason for the applicability of material damage parameters identified by SPT in the tensile-shear combine test. However, the stress condition in the pure shear testing is totally different, which results in the inapplicability the identified material parameters by SPT.
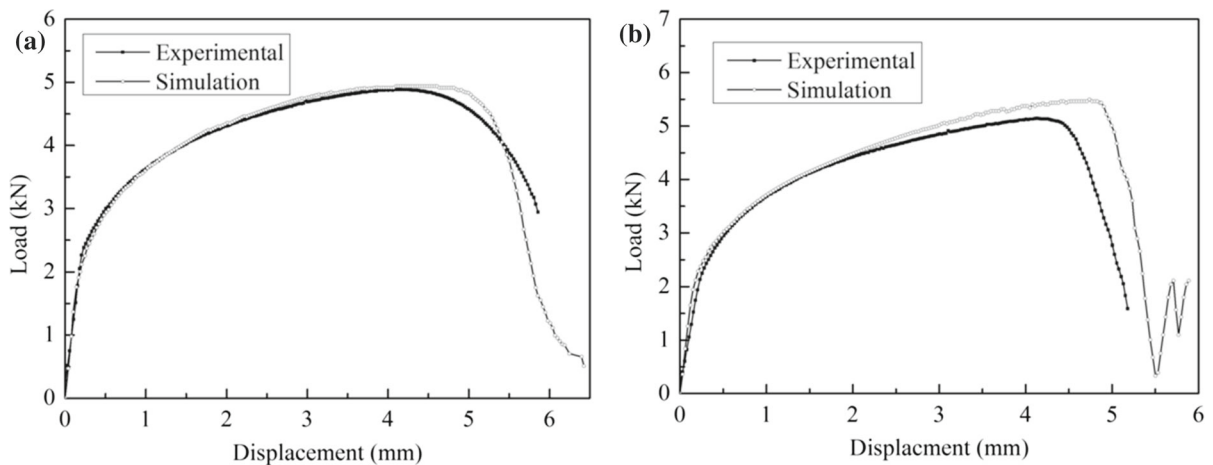
Fig. 14 Comparison of simulation and experimental results of **a** tensile-shear combine testing and **b** pure shear testing

It should be noticed that the identification of the material damage parameters of the shear modified GTN damage model in this work was based on inverse method which just fit the macroscopic load-displacement curve rather than the description of microscopic damage and fracture behavior of material. Therefore, a further verification of the identified damage parameters should be performed when they are used in other material tests with different stress conditions.

6 Conclusion

The material damage parameters of the shear modified GTN damage model is identified by the inverse method based on artificial neural networks method combined with fractional factorial design analysis. As the damage model contains seven parameters (f_0, f_N, ε_N, S_N, k_s, f_c, f_F) to be determined, the fractional factorial design analysis was conducted to recognize the most important parameters that affect the material macroscopic mechanical behavior. The fractional factorial design analysis demonstrates that the damage evolution parameters of f_N, ε_N and k_s are the significant factors that affect the mechanical behavior of specimen in SPT while the effect of f_0 and S_N is not statistically significant. An artificial neural networks model was built to identify the important damage evolution parameters of f_N, ε_N, k_s and failure parameters of f_c, f_F. The validity of the identified material damage parameters was confirmed by SPT simulations with different specimen thickness. In addition, the verifica-

tion of the applicability of the identified parameters in tensile-shear combine testing and pure shear testing come the conclusion that parameters obtained by a specific testing with inverse method may not be applicable to ones with different stress conditions and further verification should be performed when they are used.

References

Abbassi F, Belhadj T, Mistou S et al (2013) Parameter identification of a mechanical ductile damage using artificial neural networks in sheet metal forming. Mater Design 45:605–615. https://doi.org/10.1016/j.matdes.2012.09.032

Abendroth M, Kuna M (2003) Determination of deformation and failure properties of ductile materials by means of the small punch test and neural networks. Comput Mater Sci 28:633–644

Abendroth M, Kuna M (2006) Identification of ductile damage and fracture parameters from the small punch test using neural networks. Eng Fract Mech 73:710–725

Achouri M, Germain G, Dal Santo P et al (2013) Numerical integration of an advanced Gurson model for shear loading: application to the blanking process. Comput Mater Sci 72:62–67. https://doi.org/10.1016/j.commatsci.2013.01.035

Ag F (1969) Comparison between a quantitative microscope and chemical methods for assessment of non-metallic inclusions. J Iron Steel Inst 207:181–186

Aguir H, Marouani H (2010) Gurson–Tvergaard–Needleman parameters identification using artificial neural networks in

sheet metal blanking. Int J Mater Form 3:113–116. https://doi.org/10.1007/s12289-010-0720-5

Barsoum I, Faleskog J (2007) Rupture mechanisms in combined tension and shear—micromechanics. Int J Solids Struct 44:5481–5498. https://doi.org/10.1016/j.ijsolstr.2007.01.010

Benseddiq N, Imad A (2008) A ductile fracture analysis using a local damage model. Int J Press Vessels Pip 85:219–227. https://doi.org/10.1016/j.ijpvp.2007.09.003

Corigliano A, Mariani S, Orsatti B (2000) Identification of Gurson–Tvergaard material model parameters via Kalman filtering technique. I. Theory. Int J Fract 104:349–373. https://doi.org/10.1023/a:1007602106711

Cuesta II, Alegre JM, Lacalle R (2010) Determination of the Gurson–Tvergaard damage model parameters for simulating small punch tests. Fatig Fract Eng Mater Struct 33:703–713. https://doi.org/10.1111/j.1460-2695.2010.01481.x

Gurson AL (1977) Continuum theory of ductile rupture by void nucleation and growth, Part I. Yield criteria and flow rules for porous ductile media. J Eng Mater Technol 99:2–15

Marouani H, Aguir H (2012) Identification of material parameters of the Gurson–Tvergaard–Needleman damage law by combined experimental, numerical sheet metal blanking techniques and artificial neural networks approach. Int J Mater Form 5:147–155

Muñoz-Rojas P, Cardoso E, Vaz M (2010) Parameter identification of damage models using genetic algorithms. Exp Mech 50:627–634. https://doi.org/10.1007/s11340-009-9321-y

Nahshon K, Hutchinson JW (2008) Modification of the Gurson model for shear failure. Eur J Mech Solid 27:1–17. https://doi.org/10.1016/j.euromechso1.2007.08.002

Nahshon K, Xue Z (2009) A modified Gurson model and its application to punch-out experiments. Eng Fract Mech 76:997–1009. https://doi.org/10.1016/j.engfracmech.2009.01.003

Springmann M, Kuna M (2005) Identification of material parameters of the Gurson–Tvergaard–Needleman model by combined experimental and numerical techniques. Comput Mater Sci 32:544–552. https://doi.org/10.1016/j.commatsci.2004.09.010

Springmann M, Kuna M (2006) Determination of ductile damage parameters by local deformation fields: measurement and simulation. Arch Appl Mech 75:775–797

Tvergaard V (1981) Influence of voids on shear band instabilities under plane strain conditions. Int J Fract 17:389–407. https://doi.org/10.1007/bf00036191

Tvergaard V (1982) On localization in ductile materials containing spherical voids. Int J Fract 18:237–252. https://doi.org/10.1007/bf00015686

Tvergaard V, Needleman A (1984) Analysis of the cup-cone fracture in a round tensile bar. Acta Metallurgica 32:157–169